

# Novel preparation of Fe<sub>3</sub>O<sub>4</sub>/styrene-co-butyl acrylate composite microspheres via a phase inversion emulsion process

Yufeng Duan<sup>1</sup>

Received: 28 February 2017 / Revised: 9 June 2017 / Accepted: 5 July 2017 / Published online: 16 July 2017  
© Springer-Verlag GmbH Germany 2017

**Abstract** A new approach to prepare the magnetic composite microspheres of Fe<sub>3</sub>O<sub>4</sub> and copolymer of styrene-co-butyl acrylate was reported by a phase inversion emulsion technique. During the phase inversion process, the system converts from a continuous bulk organic phase to a continuous aqueous phase dispersed with organic drops composed of monomers, polymers, and Fe<sub>3</sub>O<sub>4</sub> particles. The obtained Fe<sub>3</sub>O<sub>4</sub>/styrene-co-butyl acrylate composite microspheres were mostly spherical with a diameter in the range of a few micrometers to dozens of micrometers. Also, large amounts of Fe<sub>3</sub>O<sub>4</sub> particles present in the interior of the microspheres and some were embedded in the surface. The results from X-ray powder diffraction indicated the crystal structure of Fe<sub>3</sub>O<sub>4</sub> was not changed during the preparation of microspheres. According to TGA curve, the content of Fe<sub>3</sub>O<sub>4</sub> particles in microspheres reached approximately 48%. The microspheres exhibited superparamagnetism. High-magnetic-content microspheres can be easily obtained by this method.

**Keywords** Microspheres · Phase inversion · Magnetic materials · Composites · Emulsions

## Introduction

Magnetic composite microspheres composed of magnetic materials and polymer have been attracting a great deal of

attention due to their extensive application in the fields of biomedicine [1–7], food safety detection [8], waste water treatment [9, 10], oil spill recover [11, 12], catalyst [13], toner of laser printing and xerography [14], and so on. Various approaches have been invented to prepare magnetic polymeric particles. The common route and extensive study for synthesizing magnetic composite microspheres is monomer polymerization, mainly including suspension polymerization [15], dispersion polymerization [16], emulsion polymerization [17], Pickering emulsion polymerization [18, 19], mini-emulsion polymerization [20–24], and inverse emulsion polymerization [7, 25, 26].

Among these methods, mini-emulsion polymerization has been found to be a particularly attractive way to obtain nano-composite particles and is subject to numerous theoretical and experimental studies [20–26]. Mini-emulsion polymerization is a process in which a liquid monomer (or a solution of the monomer) is dispersed into a continuous phase using (1) a high-energy-input process, such as ultrasounds and high shear rate, (2) a surfactant, and (3) a compound that is dissolved in the droplets and exhibits extra-low solubility in the continuous phase [25]. The typical method of preparing magnetic polymeric particles based on mini-emulsion polymerization is to suspend magnetic particles in the dispersed phase and then polymerize the monomer in the presence of the magnetic particles to form magnetic polymeric particles. As mini-emulsion polymerization is carried out in a nonaqueous solvent, the polymerization is called water-in-oil (W/O) or inverse (mini)emulsion polymerization [25].

Traditional inverse emulsion polymerization is a widely applied technology for the preparation of high-molecular-weight water-soluble macromolecules owing to the fact that high concentration of monomers can be contained within the aqueous droplets, while maintaining a monomer/polymer latex. The traditional inverse emulsion (including mini-emulsion

✉ Yufeng Duan  
duanyufengz@163.com

<sup>1</sup> Hebei Additive Manufacturing Industrial Technology Research Institute, Hebei University of Science and Technology, Shijiazhuang, Hebei, People's Republic of China

and micro-emulsion) was usually applied to the polymerization of hydrophilic monomers, such as acrylamide, acrylic acid, methacrylic acid, and *N*-isopropylacrylamide [25]. Chen Y et al. have reported a new method to prepare Fe<sub>3</sub>O<sub>4</sub>/PSt magnetic composite nanoparticles by inverse (mini)emulsion polymerization [26]. In that inverse emulsion system, a hydrophobic monomer, styrene, was dissolved in the continuous oil phase and the water-based magnetic ferrofluid was used as a disperse phase. The solution of water-based magnetic ferrofluid is dispersed in the continuous oil phase including the monomer styrene, and by polymerization, the Fe<sub>3</sub>O<sub>4</sub>/PSt composite particles were achieved. They got magnetic composite microspheres with core-shell structure and the magnetite content is evaluated to be 21.63% [26]. However, both the mini-emulsion polymerization and inverse (mini)emulsion polymerization are difficult to make a high-magnetic-content microspheres.

In this paper, a new method to prepare magnetic Fe<sub>3</sub>O<sub>4</sub>/polymer composite microspheres is developed via a phase inversion emulsion process. The phase inversion technique is a low-energy emulsification methods making use of the chemical energy stored in the components [27–31]. That technique has been widely used in preparing wax emulsions [32–34], bituminous emulsions [30], pharmaceutical applications [27], etc. In that technique, the emulsions are obtained via a phase inversion emulsion process of water-in-oil to oil-in-water.

In present work, one oil-phase system including monomers, magnetic particles, and polymers is inverted into the oil-in-water emulsion under a high-speed agitation with the addition of emulsifiers and water. Firstly, Fe<sub>3</sub>O<sub>4</sub> particles were dispersed in the monomer mixture of styrene (St), butyl acrylate (BA), and initiator to polymerize for a period of time. Afterward, a mixture of tween-80 and span-80 was added. Then, by adding water under a high-speed agitation, the oil phase in water emulsion was obtained. In the emulsion, spherical organic drops containing a mixture of monomers, polymers, and Fe<sub>3</sub>O<sub>4</sub> particles were dispersed in a continuous aqueous phase. Finally, the composite microspheres of Fe<sub>3</sub>O<sub>4</sub> and styrene-co-butyl acrylate (Fe<sub>3</sub>O<sub>4</sub>/P(St-BA)) were achieved, in which structures of Fe<sub>3</sub>O<sub>4</sub> particles both dispersed in microspheres homogeneously and embedded in surface. Compared with other methods, this approach is able to prepare microspheres with relatively high magnetic content easily and the process is simple. Potential advantage of this method is that almost any oil-soluble vinyl compound and any inorganic particles may be used in the same way to prepare polymer-inorganic composite microspheres. Therefore, by this way, it is easy to change the surface function group to improve the biocompatibility and adsorption of composite microspheres via selecting different monomers.

## Experiment

### Materials

Styrene and butyl acrylate were purchased from Tianjin Yongda Chemical Reagent Development Center. 2, 2'-Azobis(isobutyronitrile) (AIBN) was purchased from Tianjin Bodi Chemical Co. Ltd. Fe<sub>3</sub>O<sub>4</sub> particles were supplied by Bayer AG, E8706. Tween-80 and span-80 were also from Tianjin Yongda Chemical Reagent Development Center. Polyvinyl alcohol (PVA) was offered by Beijing Chemical Reagent Co. The water used throughout the work was deionized water.

### Preparation of Fe<sub>3</sub>O<sub>4</sub>/P(St-BA) microspheres

Fe<sub>3</sub>O<sub>4</sub>/P(St-BA) microspheres were prepared in following procedures: first, 15 g of Fe<sub>3</sub>O<sub>4</sub> particles were dispersed in a mixture of 36 and 7.2 g of BA with ultrasonic vibration and stirring for 20 min. During ultrasonication, the mixture was cooled in an ice-bath to avoid polymerization. Afterwards, 1.3 g of AIBN was charged and dissolved; the mixture was poured into a 500-ml three-neck flask equipped with a paddle blade, a reflux condenser, and a thermal probe. The mixture in reactor was heated to 70 °C in water bath at a controlled rate about 0.5 °C/min, with a stirred speed of 350–400 rpm. After a period of polymerization at 70 °C, a mixture of tween-80 (8.1 g) and span-80 (0.9 g) was added. Twenty minutes later, 0.22 g of PVA 1788 dissolved in 220 g of hot water (90 °C) was quickly added into the reactor under high stirring speed of 1000 rpm. After 20 min, the stirring speed was lowered to 350–400 rpm again. The polymerization was performed at 75 °C for another 5 h. The obtained black magnetic particles were separated from the aqueous mixture by filtration, washed with water, and then dried under vacuum.

### Characterization

The surface profile of Fe<sub>3</sub>O<sub>4</sub>/P(St-BA) composite microspheres was observed with a field emission scanning electron microscope (SEM) (S-4800, Hitachi). The internal microstructure of microspheres was investigated by observing the ultrathin sections of microspheres embedded in epoxy resin under a transmission electron microscope (TEM) (H7650, Hitachi). An optical microscope (XP-300, equipped with a graph capture device, Caikon Optical Instrument Co. Ltd.) also was used to analyze the distribution of Fe<sub>3</sub>O<sub>4</sub> particles in the microspheres. The surface tension of monomer mixtures was determined via du Nouy ring technique (JYW-200A, Chengde Dahua Test Instrument Co. Ltd.). The viscosity was measured by a rotational viscosimeter (DV3TLVTJ0, Brookfield). An X-ray powder diffraction (D/MAX 2500,

Rigaku) using Cu  $K_{\alpha}$  ( $\lambda = 1.5418 \text{ \AA}$ ) radiation was employed to analyze the crystal structure. Thermogravimetric analysis (TGA) was performed on a simultaneous TGA/DSC instrument (SDT Q600) at a heating rate of  $10 \text{ }^{\circ}\text{C}/\text{min}$  from 30 to  $1000 \text{ }^{\circ}\text{C}$  under atmosphere of  $\text{N}_2$ . A vibrating-sample magnetometer (VSM) (Model 6000, Quantum Design) was used at 300 K to measure the magnetic moment.

## Results and discussion

### Mechanism of preparing $\text{Fe}_3\text{O}_4/\text{P}(\text{St-BA})$ composite microspheres via a phase inversion emulsion process

The synthesis procedure for  $\text{Fe}_3\text{O}_4/\text{P}(\text{St-BA})$  microspheres in this work was shown in Scheme 1. Firstly,  $\text{Fe}_3\text{O}_4$  particles were ultrasonically dispersed in an AIBN-dissolved monomer mixture of St and BA. The reactor was heated to  $70 \text{ }^{\circ}\text{C}$  at a controlled rate and kept constant to perform polymerization (Scheme 1a). The emulsifier mixture of tween-80 and span-80 was then slowly added. After 20 min, the aqueous solution dissolved with PVA was quickly poured into the reactor under a high-speed stirring. During the process, phase inversion occurred. The system turned to a continuous aqueous phase dispersed with spherical organic drops composed of monomers, polymers, and  $\text{Fe}_3\text{O}_4$  particles (Scheme 1b). After completing the polymerization, the black  $\text{Fe}_3\text{O}_4/\text{P}(\text{St-BA})$  microspheres were separated from the aqueous mixture (Scheme 1c).

During the preparation process,  $\text{Fe}_3\text{O}_4$  particles were firstly dispersed in the mixture of St and BA. So St and BA can be used as the monomers of polymerization and the dispersion medium of  $\text{Fe}_3\text{O}_4$  particles. During that course, the solid-gas interfaces between  $\text{Fe}_3\text{O}_4$  particles and air were replaced by solid-liquid interface between  $\text{Fe}_3\text{O}_4$  particles and monomer mixture. So a surface free energy change was formed in this system.

In the system, the “work of adhesion,”  $W_a$ , is the decrease in Helmholtz free energy of the whole system

due to the interactions between  $\text{Fe}_3\text{O}_4$  particles and monomer mixture, i.e.,

$$W_a = \gamma_{\text{Fe}_3\text{O}_4} + \gamma_{\text{monomers}} - \gamma_{\text{Fe}_3\text{O}_4/\text{monomers}}, \quad (1)$$

where  $\gamma_{\text{Fe}_3\text{O}_4}$  is the surface tension of  $\text{Fe}_3\text{O}_4$  particles,  $\gamma_{\text{monomers}}$  is the surface tension of monomer mixture, and  $\gamma_{\text{Fe}_3\text{O}_4/\text{monomers}}$  is the interfacial tension between  $\text{Fe}_3\text{O}_4$  particles and monomer mixture.  $W_a$  also represents the work necessarily to separate the  $\text{Fe}_3\text{O}_4$  particles from monomers mixture at interface.

Good and Girifalco [35] developed a general expression for the interfacial energy,  $\gamma_{\text{AB}}$ , between two phases A and B in terms of the respective pure component surface tension,  $\gamma_A$  and  $\gamma_B$ :

$$\gamma_{\text{AB}} = \gamma_A + \gamma_B - 2\phi(\gamma_A\gamma_B)^{1/2}. \quad (2)$$

$\phi$  is a parameter, expressing the degree of departure from the geometric mean assumption.

Applying Eq. (2) to the system in the work in this paper, the following equation can be deduced:

$$\gamma_{\text{Fe}_3\text{O}_4/\text{monomers}} = \gamma_{\text{Fe}_3\text{O}_4} + \gamma_{\text{monomers}} - 2\phi(\gamma_{\text{Fe}_3\text{O}_4}\gamma_{\text{monomers}})^{1/2}. \quad (3)$$

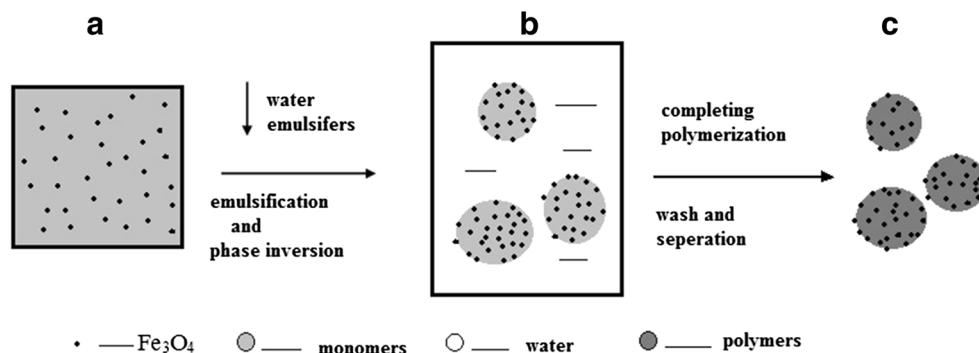
Therefore, from Eqs. (1) and (3), for a system of  $\text{Fe}_3\text{O}_4$  particles dispersed in monomer mixtures,

$$W_a = 2\phi(\gamma_{\text{Fe}_3\text{O}_4}\gamma_{\text{monomers}})^{1/2}. \quad (4)$$

Equation (4) shows that as the surface tension of monomer mixture increases, the “work of adhesion” between  $\text{Fe}_3\text{O}_4$  particles and monomer mixture becomes greater.

In this work, the polymerization of St and BA happened when  $\text{Fe}_3\text{O}_4$  particles were dispersed into mixture of St and BA in which the initiator was charged. With the performing of polymerization, the substances in reactor gradually changed from a mixture of a small molecular monomers and  $\text{Fe}_3\text{O}_4$

**Scheme 1** Schematic illustration for the preparation of  $\text{Fe}_3\text{O}_4/\text{P}(\text{St-BA})$  microspheres via phase inversion



particles to a mixture of polymer-dissolved monomers and  $\text{Fe}_3\text{O}_4$  particles. In the process, the surface tension and viscosity of the system becomes greater with the increase of time (Table 1). From Table 1, it can be seen that the surface tension of monomer phase,  $\gamma_{\text{monomers}}$ , gradually increases with the advance of polymerization times. Therefore, it can be deduced that the adhesion between  $\text{Fe}_3\text{O}_4$  particles and polymer-dissolved monomers becomes more and more tightly with the increase of time as the “work of adhesion” between  $\text{Fe}_3\text{O}_4$  particles and monomer mixture,  $W_a$ , is proportional to  $\gamma_{\text{monomers}}$  (Eq. 4). So it can be assumed that more  $\text{Fe}_3\text{O}_4$  particles would be maintained in the polymer-dissolved monomer drops during later phase inversion process when the polymerization before the phase inversion lasts for a longer time. Meanwhile, the increased viscosity also greatly retarded the fleeing of  $\text{Fe}_3\text{O}_4$  particles from the polymer-dissolved monomer drops. In addition, some long-chain polymers may enwrap the  $\text{Fe}_3\text{O}_4$  particles and obstruct the fleeing of the  $\text{Fe}_3\text{O}_4$  particles from the polymer-dissolved monomer drops to aqueous phase during the phase inversion process.

Figure 1a–c exhibited optical microscope images of  $\text{Fe}_3\text{O}_4/\text{P}(\text{St-BA})$  microspheres fabricated by phase inversion method at different polymerization times of 20, 40, and 80 min, respectively. Figure 1a showed that only a few  $\text{Fe}_3\text{O}_4$  particles were encapsulated in polymers, while most of  $\text{Fe}_3\text{O}_4$  particles were fled from polymer/monomer drops to water in the process of phase inversion. When the phase inversion was carried out after a longer polymerization time of 40 or 80 min, the amount of  $\text{Fe}_3\text{O}_4$  particles encapsulated in microspheres increased (Fig. 1b, c). One reason is that the interface adhesion formed by intermolecular forces between  $\text{Fe}_3\text{O}_4$  particles and polymer-dissolved monomers increased with the advance of polymerization (according to Eq. (4)), since the gradually increasing amount of polymers in monomer phase gave rise to rising surface tension of monomer phase,  $\gamma_{\text{monomers}}$ . In addition, the increased viscosity of monomer phase and the greater entanglements of the polymer chains on the  $\text{Fe}_3\text{O}_4$  particles also retarded fleeing of the  $\text{Fe}_3\text{O}_4$  particles from

monomer drops to aqueous phase. As a result, with the advance of polymerization, it was increasingly hard for the  $\text{Fe}_3\text{O}_4$  particles to break away from the polymer-dissolved monomer drops during the following phase inversion process. So the amount of encapsulated  $\text{Fe}_3\text{O}_4$  particles in the obtained microspheres elevated when the polymerization time before phase inverse process increased from 20 to 40 and 80 min. It was noted that the phase inversion became very difficult when the polymerization time exceeded 90 min because of excessively high viscosity of polymer-dissolved monomer bulk phase.

### Determination of operating conditions for phase inversion emulsion process

In this method, the composite microspheres are obtained via a phase inversion emulsion process of water-in-oil to oil-in-water. Therefore, the effect factors on the microsphere's size and size distribution mainly include HLB value, surfactant concentration, temperature and emulsification route, stirring rate, and the ratio of water to oil, which are similar to a typical phase inversion process of water-in-oil to oil-in-water [32, 34, 36, 37].

Usually, stable emulsions of oil in water are formed at the presence of the emulsifiers or their combination with a HLB value close to that required of oil phase [28, 29]. Here, the oil phase is composed of monomer styrene, butyl acrylate, and  $\text{Fe}_3\text{O}_4$  particles. The approximate HLB value of the oil phase can be calculated by the following Eq. (5):

$$\text{HLB}_{\text{oil}} = \text{HLB}_{\text{Styrene}} \times \text{Styrene}\% + \text{HLB}_{\text{BA}} \times \text{BA}\%, \quad (5)$$

where  $\text{HLB}_{\text{oil}}$ ,  $\text{HLB}_{\text{Styrene}}$ , and  $\text{HLB}_{\text{BA}}$  are the calculated HLB values of oil phase, required HLB values of polystyrene emulsion (13.0–16.0) [38], and required HLB values of polybutyl acrylate emulsion (14.5–15.5 [32], respectively.  $\text{Styrene}\%$  and  $\text{BA}\%$  are the mass percentages of styrene and butyl acrylate in the mixed monomers. In this work, the mass ratio of styrene to butyl acrylate was 5:1. The calculated value of  $\text{HLB}_{\text{oil}}$  was 13.25–15.91.

To attain the more stable droplet, the combination of hydrophilic and hydrophobic emulsifiers is often utilized, which was considered to align alongside each other imparting more rigidity and strength to the emulsifier film [32, 36]. In this work, emulsifier blend was prepared with 90 wt% tween-80 and 10 wt% span-80. The mixed HLB value of emulsifier blend was calculated by the following Eq. (6):

$$\text{HLB}_{\text{emulsifier blend}} = \text{HLB}_{\text{tween-80}} \times \text{tween}\% + \text{HLB}_{\text{span-80}} \times \text{span}\%, \quad (6)$$

where  $\text{HLB}_{\text{emulsifier blend}}$ ,  $\text{HLB}_{\text{tween-80}}$ , and  $\text{HLB}_{\text{span-80}}$  are the HLB values of the emulsifier blend, tween-80 (15.0), and

**Table 1** Test values for surface tension and viscosity of monomer mixtures at different polymerization times (before performing phase inversion, 20 °C)

Sample	Polymerization time (min)	Surface tension ( $\text{mN}\cdot\text{m}^{-1}$ )	Viscosity ( $\text{mPa}\cdot\text{s}$ )
1	0	33.1	–
2	20	36.8	22.5
3	40	37.8	50.0
4	80	39.3	70.0
5	90	39.5	107.5



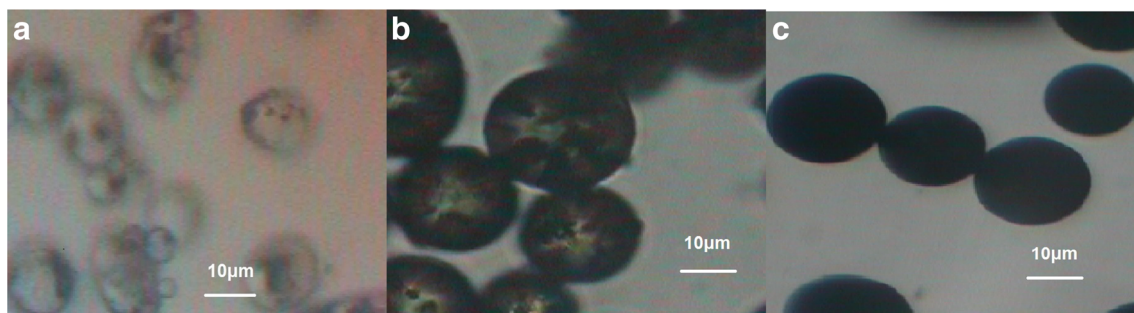


**Fig. 1** Optical microscope images of  $\text{Fe}_3\text{O}_4/\text{P}(\text{St-BA})$  microspheres prepared by performing phase inversion at different polymerization times of 20 min (a), 40 min (b), and 80 min (c)

span-80 (4.3), respectively. The tween% and span% are the mass percentages of tween-80 and span-80 in the emulsifier blend. The calculated value of  $\text{HLB}_{\text{emulsifier blend}}$  was 14.36.

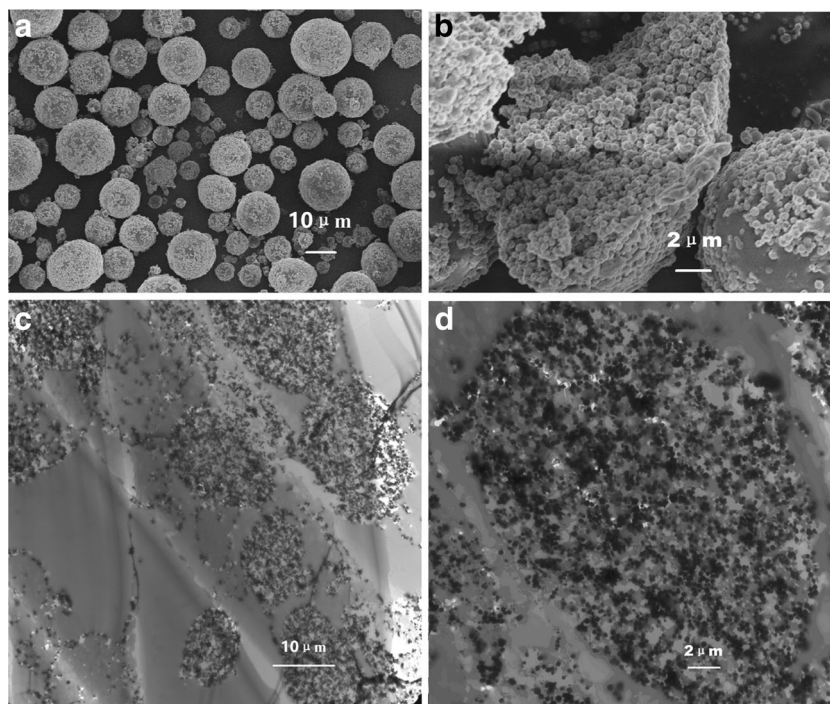
Considering the facts that the decomposition temperature of initiator AIBN is 45–80 °C and span-80 can be dissolved in hot water, the temperature of phase inversion process is set at 70 °C. The microsphere's size declined with the increase of the surfactant concentration, stirring rate, and ratio of water, which is consistent with rules of typical phase inversion [32, 34, 37]. Here, the surfactant concentration is about 20 wt% of the monomers. The stirring rate during phase inversion is set at 1000 rpm. The ratio between water and monomers is 5 to 1.

Considering the viscosity of oil drops increasing with the gradual advance of polymerization, 0.1 wt% of PVA 1788 was dissolved in the water to prevent the drops from coalescing during polymerization process.

### Microstructure of $\text{Fe}_3\text{O}_4/\text{P}(\text{St-BA})$ composite microspheres prepared via phase inversion process

SEM and TEM images of  $\text{Fe}_3\text{O}_4/\text{P}(\text{St-BA})$  microspheres (prepared by performing phase inversion after polymerization 80 min) were shown in Fig. 2. As shown in Fig. 2a, the majority of the  $\text{Fe}_3\text{O}_4/\text{P}(\text{St-BA})$  particles were spherical in shape, accompanied with a few ellipsoidal microspheres. The size of  $\text{Fe}_3\text{O}_4/\text{P}(\text{St-BA})$  microspheres ranged from a few microns to dozens of microns. Figure 2b showed one of typical broken microspheres, which was deliberately crushed at low temperature (−30 °C) before observation. The two images both showed that many  $\text{Fe}_3\text{O}_4$  particles were embedded in the interior of the microspheres, and some  $\text{Fe}_3\text{O}_4$  particles were embedded in the surface. Internal microstructure of  $\text{Fe}_3\text{O}_4/\text{P}(\text{St-BA})$  microspheres was also investigated by TEM (Fig. 2c, d). The close-up images (Fig. 2d) clearly illustrated that large amounts of  $\text{Fe}_3\text{O}_4$  particles were encapsulated by polymers.

**Fig. 2** SEM images (a, b) and TEM images (c, e) of  $\text{Fe}_3\text{O}_4/\text{P}(\text{St-BA})$  microspheres



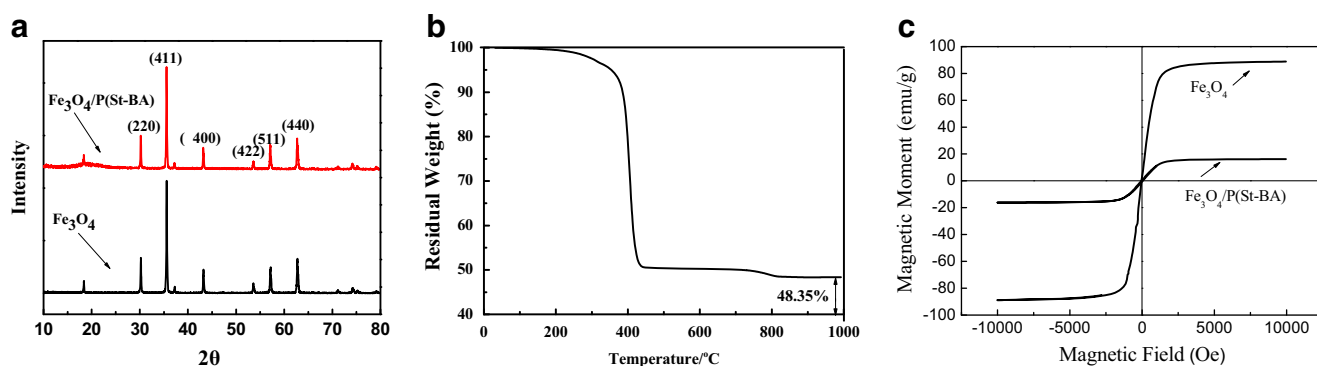


**Fig. 3** **a** X-ray diffraction patterns of  $\text{Fe}_3\text{O}_4$  particles and  $\text{Fe}_3\text{O}_4/\text{P}(\text{St-BA})$  microspheres; **b** TGA curve of  $\text{Fe}_3\text{O}_4/\text{P}(\text{St-BA})$  microspheres; **c** magnetic hysteresis loops of  $\text{Fe}_3\text{O}_4$  particles and  $\text{Fe}_3\text{O}_4/\text{P}(\text{St-BA})$  microspheres

### Characterization of $\text{Fe}_3\text{O}_4/\text{P}(\text{St-BA})$ composite microspheres prepared via phase inversion process

The crystal structure of  $\text{Fe}_3\text{O}_4$  particles and  $\text{Fe}_3\text{O}_4/\text{P}(\text{St-BA})$  microspheres were characterized by X-ray diffraction, shown in Fig. 3a. For the  $\text{Fe}_3\text{O}_4$  particles, the diffraction peaks at  $2\theta$  of  $30.206^\circ$ ,  $35.565^\circ$ ,  $43.199^\circ$ ,  $53.579^\circ$ ,  $57.121^\circ$ , and  $62.734^\circ$  were corresponding to the inverse spinel structure of  $\text{Fe}_3\text{O}_4$  [8]. These peaks were ascribed to the diffraction faces of the crystals at (220), (311), (400), (422), (511), and (440), respectively. The peak position of  $\text{Fe}_3\text{O}_4$  particles was unchanged before and after encapsulation by P(St-BA). This result indicated that the crystal structure of  $\text{Fe}_3\text{O}_4$  is not changed during the preparation of microspheres. The broad diffraction peaks of  $\text{Fe}_3\text{O}_4/\text{P}(\text{St-BA})$  microspheres between  $10^\circ$  and  $30^\circ$  were attributed to the amorphous polymer in the microspheres.

Figure 3b showed the TGA curve of  $\text{Fe}_3\text{O}_4/\text{P}(\text{St-BA})$  microspheres. The weight loss at  $150\text{--}300^\circ\text{C}$  was due to the decomposition of residual surfactants. The major weight loss transition of  $\text{Fe}_3\text{O}_4/\text{P}(\text{St-BA})$  composite microspheres occurred between  $310$  and  $430^\circ\text{C}$  with a weight loss of  $49.62\%$  due to the removal of the P(St-BA). At temperature above  $500^\circ\text{C}$ , the P(St-BA) was almost decomposed. The small weight loss ( $1.44\%$ ) from  $600$  to  $800^\circ\text{C}$  was related to the decomposition of carbon due to carbonization of polymers. The residual weight above  $900^\circ\text{C}$  should be the weight of  $\text{Fe}_3\text{O}_4$ . According to the TGA curve, the magnetite content of  $\text{Fe}_3\text{O}_4$  particles in microspheres is evaluated to be more than  $48\%$ . That result indicated that high-magnetic-content microspheres can be easily obtained by the method described in this paper.

The magnetism of  $\text{Fe}_3\text{O}_4$  and  $\text{Fe}_3\text{O}_4/\text{P}(\text{St-BA})$  microspheres was measured by VSM. Field dependence hysteresis loops of  $\text{Fe}_3\text{O}_4$  and  $\text{Fe}_3\text{O}_4/\text{P}(\text{St-BA})$  microspheres were presented in Fig. 3c. It can be seen that the hysteresis and the coercivity were almost undetectable, indicating that the  $\text{Fe}_3\text{O}_4/\text{P}(\text{St-BA})$  microspheres are superparamagnetic. The saturation magnetization of  $\text{Fe}_3\text{O}_4$  and  $\text{Fe}_3\text{O}_4/\text{P}(\text{St-BA})$  microspheres was  $88.83$  and  $16.17$  emu/g, respectively.

### Conclusion

A new approach was developed to prepare  $\text{Fe}_3\text{O}_4/\text{P}(\text{St-BA})$  microspheres based on the methods of phase inverse polymerization by converting a continuous organic bulk phase containing monomers, polymers, and  $\text{Fe}_3\text{O}_4$  particles to a continuous aqueous phase with spherical organic drops. The obtained  $\text{Fe}_3\text{O}_4/\text{P}(\text{St-BA})$  particles were mostly spherical with a diameter from a few micrometers to dozens of micrometers range. Large amounts of  $\text{Fe}_3\text{O}_4$  particles were found in the interior of the microspheres and some were embedded in the surface. The content of  $\text{Fe}_3\text{O}_4$  particles in microspheres reached approximately  $48\%$ . The microspheres exhibited superparamagnetism. High-magnetic-content microspheres can be easily obtained by this method.

**Acknowledgments** This work was supported by the Science and Technology Research Key Project Foundation of Hebei Provincial Department of Education (ZD2014102) and the Open Project Foundation of Hebei Additive Manufacturing Industrial Technology Research Institute (Hebei University of Science and Technology).

### Compliance with ethical standards

**Conflict of interest** The author declares that she has no conflict of interest.

### References

- Koc K, Alveroglu E (2015) Adsorption and desorption studies of lysozyme by  $\text{Fe}_3\text{O}_4$ -polymer nanocomposite via fluorescence spectroscopy *J Mol Struct* 1089:66–72
- Ladj R, Bitar A, Mohamed ME, et al. (2013) Polymer encapsulation of inorganic nanoparticles for biomedical applications *Int J Pharm* 458(1):230–241
- Horák D, Španová A, Tvrdíková J, et al. (2011) Streptavidin-modified magnetic poly(2-hydroxyethyl methacrylate-co-glycidyl methacrylate) microspheres for selective isolation of bacterial DNA *Eur Polym J* 47(5):1090–1096

4. Veisoh O, Gunn JW (2010) Design and fabrication of magnetic nanoparticles for targeted drug delivery and imaging *Adv Drug Deliv Rev* 62(3):284–304
5. Kuan W, Horák D, Plichta Z, et al. (2014) Immunocapture of CD133-positive cells from human cancer cell lines by using monodisperse magnetic poly(glycidyl methacrylate) microspheres containing amino groups *Mater Sci Eng C* 34(1):193–200
6. Zhao D, Huang W, Rahaman N, et al. (2012) Preparation and characterization of composite microspheres for brachytherapy and hyperthermia treatment of cancer *Mater Sci Eng C* 32(2):276–281
7. Zhang B, Zhang H, Li X (2013) Synthesis of BSA/Fe<sub>3</sub>O<sub>4</sub> magnetic composite microspheres for adsorption of antibiotics *Mater Sci Eng C* 33:4401–4408
8. Tang D, Saucedo JC, Lin Z, et al. (2009) Magnetic nanogold microspheres-based lateral-flow immunodip stick for rapid detection of aflatoxin B<sub>2</sub> in food *Biosens Bioelectron* 25(2):514–518
9. Park J, Jang I, Kang Y, et al. (2014) Morphology-controlled synthesis of polystyrene-Mn<sub>3</sub>O<sub>4</sub> nanocomposites using surfactant and their application for water treatment *Colloids Surf A Physicochem Eng Asp* 441:340–345
10. Zhang M, Zhou Q, Li A, et al. (2013) A magnetic sorbent for the efficient and rapid extraction of organic micropollutants from large-volume environmental water samples *J Chromatogr A* 1316(5):44–52
11. Mao J, Jiang W, Gu J, et al. (2014) Synthesis of P (St-DVB)/Fe<sub>3</sub>O<sub>4</sub> microspheres and application for oil removal in aqueous environment *Appl Surf Sci* 317:787–793
12. Yu L, Hao G, Gu J, et al. (2015) Fe<sub>3</sub>O<sub>4</sub>/PS magnetic nano particles: synthesis, characterization and their application as sorbents of oil from waste water *J Magn Magn Mater* 394:14–21
13. Yuan D, Chen L, Yuan L, et al. (2016) Superparamagnetic polymer composite microspheres supported Schiff base palladium complex: an efficient and reusable catalyst for the Suzuki coupling reactions *Chem Eng J* 287:241–251
14. Hasegawa J, Yanagida N, Tamura M (1999) Toner prepared by the direct polymerization method in comparison with the pulverization method *Colloids and Surfaces A: Physicochemical and Engineering Aspects* 153:215–220
15. Liu H, Wang C, Gao Q, et al. (2010) Magnetic hydrogels with supracolloidal structures prepared by suspension polymerization stabilized by Fe<sub>2</sub>O<sub>3</sub> nanoparticles *Acta Biomater* 6:275–281
16. Donescu D, Raditoiu V, Spataru CI, et al. (2012) Superparamagnetic magnetite-divinylbenzene-maleic anhydride copolymer nanocomposites obtained by dispersion polymerization *Eur Polym J* 48:1709–1716
17. Chen H, Wang W, Li G, et al. (2011) Synthesis of PST-MMA-Fe<sub>3</sub>O<sub>4</sub>/PPy core-shell composite microspheres with conductivity and superparamagnetic behaviors *Synth Met* 161:1921–1927
18. Yin D, Du X, Liu H, et al. (2012) Facile one-step fabrication of polymer microspheres with high magnetism and armored inorganic particles by Pickering emulsion polymerization *Colloids Surf A Physicochem Eng Asp* 414:289–295
19. Wang C, Zhang C, Li Y, et al. (2009) Facile fabrication of nanocomposite microspheres with polymer cores and magnetic shells by Pickering suspension polymerization *Reactive&Functional polymers* 69:750–754
20. Wang H, Wang R, Wang L, et al. (2011) Preparation of multi-core/single-shell OA-Fe<sub>3</sub>O<sub>4</sub>/PANI bifunctional nanoparticles via miniemulsion polymerization *Colloids Surf A Physicochem Eng Asp* 384:624–629
21. Qian Z, Zhang Z, Chen Y (2008) A novel preparation of surface-modified paramagnetic magnetite/polystyrene nanocomposite microspheres by radiation-induced miniemulsion polymerization *J Colloid Interface Sci* 327:354–361
22. Mori Y, Kawaguchi H (2007) Impact of initiators in preparing magnetic polymer particles by miniemulsion polymerization *Colloids Surf B: Biointerfaces* 56:246–254
23. Yang B, Yang J, Zhang J, et al. (2014) Facile fabrication of magnetic hybrid-shell microcapsule via miniemulsion polymerization *Mater Lett* 114(1):60–62
24. Kim Y, Lee S, Govindaiaha P, et al. (2013) Multifunctional Fe<sub>3</sub>O<sub>4</sub> nanoparticles-embedded poly(styrene)/poly(thiophene) core/shell composite particles *Synth Met* 175:56–61
25. Capek I (2010) On inverse miniemulsion polymerization of conventional water-soluble monomers *Adv Colloid Interf Sci* 156:35–61
26. Chen Y, Qian Z, Zhang Z (2008) Novel preparation of magnetite/polystyrene composite particles via inverse emulsion polymerization *Colloids Surf A Physicochem Eng Asp* 312(2–3):209–213
27. Sadurn iN, Solans C, Azemar N, et al. (2005) Studies on the formation of O/W nano-emulsions, by low-energy emulsification methods, suitable for pharmaceutical applications *Eur J Pharm Sci* 26:438–445
28. Charin RM, Araújo BC, Farias AC, et al. (2015) Studies on transitional emulsion phase inversion using the steady state protocol *Colloids Surf A Physicochem Eng Asp* 484:424–433
29. Sasaki Y, Konishi N, Kasuya M, et al. (2015) Preparation of size-controlled polymer particles by polymerization of O/W emulsion monomer droplets obtained through phase inversion temperature emulsification using amphiphilic comb-like block polymers *Colloids Surf A Physicochem Eng Asp* 482:68–78
30. Querol N, Barreneche C, Cabeza LF (2017) Method for controlling mean droplet size in the manufacture of phase inversion bituminous emulsions *Colloids Surf A* 527:49–54
31. Tadros T, Izquierdo P, Esquena J, et al. (2004) Formation and stability of nano-emulsions *Adv Colloid Interf Sci* 108–109:303–318
32. Li C, Mei Z, Liu Q, et al. (2010) Formation and properties of paraffin wax submicron emulsions prepared by the emulsion inversion point method *Colloids Surf A Physicochem Eng Asp* 356:71–77
33. Binks BP, Rocher A (2009) Effects of temperature on water-in-oil emulsions stabilised solely by wax microparticles *J Colloid Interface Sci* 335:94–104
34. Liu W, Sun D, Li C, et al. (2006) Formation and stability of paraffin oil in-water nano-emulsions prepared by the emulsion inversion point method *J Colloid Interf Sci* 303:557–563
35. Cherry BW (1981) *Polymer surface*. Cambridge University Press, Cambridge, pp. 18–19
36. Aulton ME (1995) *Pharmaceutics: the science of dosage form design*. Churchill Livingstone, New York, pp. 290–292
37. Forgiarini A, Esquena J, Gonzalez C, et al. (2001) Formation and stability of nanoemulsions in mixed nonionic surfactant systems *Progr Colloid Polym Sci* 118:84–189
38. Cao T, Liu J, Hu J (2007) *Principle of synthesis, properties and applications of polymer emulsion*, vol 149-151. second edn. Chemical Industry Press, Beijing, pp. 167–168